Applied Surface Science 302 (2014) 231–235

Contents lists available at ScienceDirect

Applied Surface Science

journal homepage: www.elsevier.com/locate/apsusc

Microstructuring of soft organic matter by temporally shaped femtosecond laser pulses

Esther Rebollar[a,*], Jutta Mildner[b], Nadine Götte[b], Dirk Otto[b], Cristian Sarpe[b], Jens Köhler[b], Matthias Wollenhaupt[b], Thomas Baumert[b], Marta Castillejo[a]

[a] Instituto de Química Física Rocasolano, IQFR-CSIC, Serrano 119, 28006 Madrid, Spain
[b] Institut für Physik, Universität Kassel, Heinrich-Plett-Str. 40, D-34132 Kassel, Germany

ARTICLE INFO

Article history:
Received 14 June 2013
Received in revised form 18 October 2013
Accepted 18 October 2013
Available online 29 October 2013

Keywords:
Femtosecond laser processing
Polymer films
Temporally shaped femtosecond pulses

ABSTRACT

Thin films of the biopolymers gelatine and chitosan were treated using femtosecond pulse shaping techniques combined with a microscope-based setup for material processing. The polymer films were irradiated with laser pulses of 35 fs and a central wavelength of 790 nm provided by an amplified Ti:Sapphire system. The effect of temporal pulse shaping, with quadratic and cubic spectral phases, on the induced morphology was analyzed by characterization of the created surface structures via scanning electron microscopy. We observed different material modification thresholds and different structure sizes for temporally asymmetric pulse shapes. The results indicate the possibility of control of the generated microstructures and are discussed in relation to the formation of free electrons and the different contributions of multi-photon and avalanche ionization processes.

1. Introduction

The generation of micro- and nanopatterns with complex morphologies remains an ambitious challenge in technology. Behind the fundamental interest in understanding the physical process, the motivation to study micro- and nanopatterning is also driven by the great potential of such structures for advanced applications in e.g. nanofluidics, nanophotonics and biomedical devices [1–3].

Biopolymers constitute important sources of novel functional materials and advantageous alternatives to synthetic polymers in biomedical applications. For those applications, both the substrate topography and the substrate chemistry have an important effect [4,5]. In order to control these properties, a variety of processing techniques such as stamping, stereo lithography, two-photon polymerization, electrospinning, polymer demixing and stencil [6–9] have been applied. However, common micro-fabrication techniques are prone to difficulties when dealing with biomaterials due to their typical non biocompatibility [7]. As an alternative, laser-based methods have been already used for porous scaffold fabrication on various materials [10–13], since they afford the sought versatility and reliability [14–17]. Recently, superficial laser foaming on films of biopolymers such as collagen and gelatine has been reported, a phenomenon that is induced by applying single pulses both in the nanosecond and femtosecond domains [14,16–21].

Lasers delivering ultrashort pulses have emerged as a unique tool for processing wide band gap materials for a variety of applications [22–24]. Materials which are transparent to light in the visible and near infrared spectral region become highly absorbing when ultrashort laser pulses of sufficient high intensity are applied. This allows material processing, but effective control of laser induced effects is required. Related to this, a large number of experiments have been devoted to the study of laser induced damage in the case of dielectrics. These involve investigations on the effect of pulse duration [25,26] and the application of double pulses [27,28], pulse trains [29] and temporally shaped asymmetric pulses [30–32].

In this work, we present experimental studies with single 35 fs pulses with temporally asymmetric shapes obtained by introducing a third-order dispersion (TOD) via spectral phase modulation, enabling the control of the effects induced on different biopolymer films. Also chirped pulses making use of group delay dispersion (GDD) (i.e. symmetric temporal pulse envelope but asymmetric instantaneous frequency) and combination of shaped pulses with GDD and TOD were tested. Our experiments reveal a systematic dependence of the surface damage threshold and of the size of the obtained structures on the phase mask applied in the case of TOD shaped pulses for the different biopolymers, while no significant differences are observed for those shaped via GDD.

* Corresponding author. Tel.: +34 915619400; fax: +34 915642431.
E-mail address: e.rebollar@iqfr.csic.es (E. Rebollar).

0169-4332/$ – see front matter © 2013 Elsevier B.V. All rights reserved.
http://dx.doi.org/10.1016/j.apsusc.2013.10.111

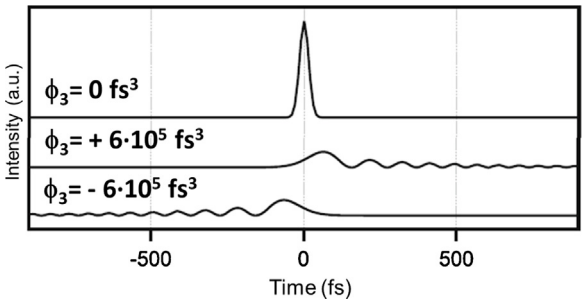

Fig. 1. Calculated temporal intensity envelopes of pulses for different values of the third order dispersion ϕ_3. Figure adapted from reference [31].

2. Experimental

Self-standing films of the biopolymers gelatine B75 (Sigma) and chitosan (Aldrich) were prepared by the method of solvent evaporation. Chitosan was solved in acetic acid 0.4 M in a concentration of 20 g/L, while gelatine was solved in water in a concentration of 12 g/L. Then, solutions were poured on Petri dishes with a diameter of 8.5 cm. The thicknesses of the resulting films are 110–180 μm. The mean roughness values (R_a) are in the range of a few nanometers as determined by atomic force microscopy (AFM).

For irradiation we combine femtosecond pulse shaping techniques [30,31,33] with a microscope setup for material processing [34]. The system was previously described in refs [30,31]. Briefly, laser pulses with Δt = 35 fs full width at half maximum (FWHM) and a central wavelength of 790 nm are provided by an amplified Ti:Sapphire laser system.

For material processing phase shaped femtosecond pulses are directed onto the different polymer films via a 50x/0.5 objective. Irradiation is carried out in defocused conditions, with a calculated diameter, taking into account a Gaussian profile, of ca. 17 μm, which corresponds to peak fluences of about 1 J/cm^2. The single shot pulse energy is adjusted by a motor-driven gradient neutral density filter and recorded with a calibrated photodiode. The sample is translated by a 3-axis piezo-table to a new position for each shot. In order to ensure that the surface is within the chosen focus position, the sample surface is probed with a HeNe laser prior to material processing.

While phase modulation does not change the spectrum of the pulse, the temporal profile is altered. By applying a TOD (ϕ_3) we obtain a train of pulses with an asymmetric time profile (see Fig. 1). Changing the sign of the ϕ_3 inverts the time profile.

Analytic formulas for cubic phase shaped laser pulses of the form $\phi(\omega) = (\phi_3/3!)(\omega - \omega_0)^3$ can be found in [31,35,36]. For each pattern, three laser pulses with the same energy and focusing conditions were used for irradiation, with values of $\phi_3 = 0$ and $\pm 6 \times 10^5$ fs^3, where $\phi_3 = 0$ corresponds to an unshaped pulse.

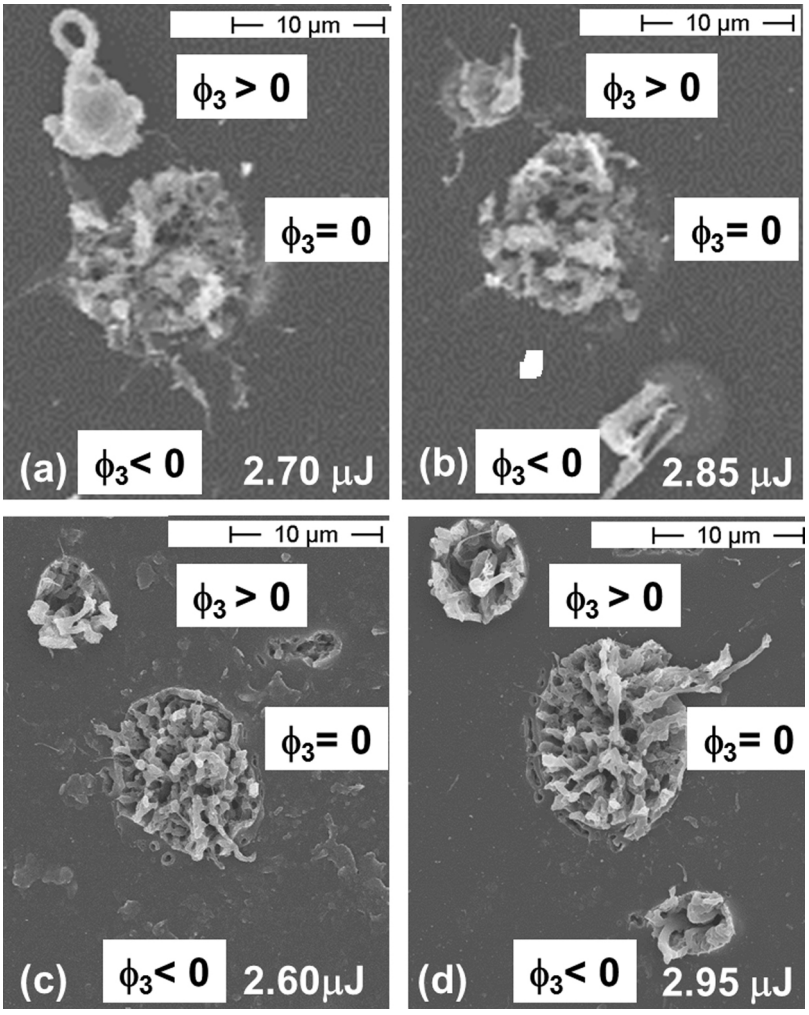

Fig. 2. SEM images of patterns obtained upon irradiation with TOD shaped pulses ($\phi_3 = 0$ (middle), $+6 \times 10^5$ fs^3 (upper) and -6×10^5 fs^3 (lower)) on gelatine (a) and (b) and chitosan films (c) and (d) at the indicated energies per pulse and same distance to focus.

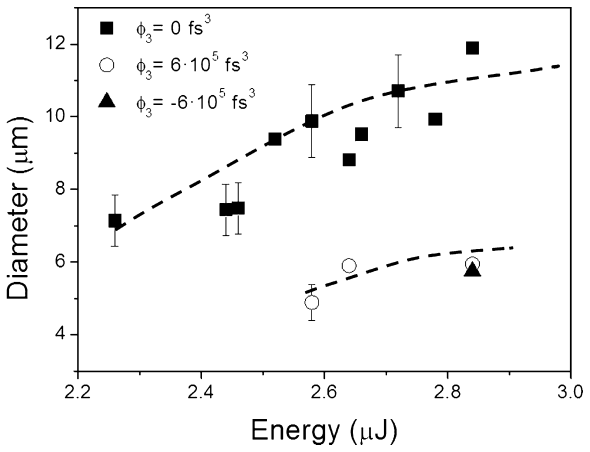

Fig. 3. Diameters of the laser modified area for a chitosan film irradiated with pulses with different values of ϕ_3. Lines are drawn to guide the eye.

Additionally, we used GDD temporally shaped pulses obtained by applying the phase masks $\phi_2 = \pm 1 \times 10^4$ fs^2, as well as shaped pulses by combination of TOD and GDD.

Analysis of the irradiated samples, previously coated with a platinum layer of ca. 3 nm thick, was carried out by Scanning Electron Microscopy (SEM, HITACHI S4000). We determined the threshold for material damage and the change of morphologies induced by laser irradiation.

3. Results

Irradiation with a single fs pulse above the modification threshold energy of the studied polymer films leads to the formation of superficial circular spots with a foamy and fibrous appearance, as reported before [14,16,17,19,21]. The modification threshold energy for unshaped pulses is around 1.2 μJ, both for chitosan and gelatine and the diameter of the laser induced structures is typically a few micrometers.

Fig. 2 shows SEM micrographs of structures obtained on gelatine (a and b) and chitosan (c and d) films. These correspond to irradiation with triplets of laser pulses with different ϕ_3 values and fixed energy and distance to focus. In each micrograph, for all ϕ_3 values, the pulses have the same energy, spectral intensity, and spatial profile. Pulses with positive and negative phase masks have the same duration but their temporal profile is time-inverted (see Fig. 1). Fig. 2 shows structures resulting from $\phi_3 = 0$ and $\pm 6 \times 10^5$ fs^3. Micrographs in Fig. 2a and c correspond to irradiation with a lower energy per pulse at the same distance to focus, i.e., lower fluence, in comparison to those shown in Fig. 2b and d.

As observed in Fig. 2, the threshold energy for ablation is higher for the pulses with negative TOD. For instance in the case of chitosan, when processing with a positive ϕ_3 value, the ablation threshold is around 2.5 μJ. For negative ϕ_3 however, modification of the surface occurs for energies higher than 2.9 μJ and the modified area has the same size than the one obtained upon irradiation with positive ϕ_3.

The dependence of the diameter of the structure with energy for the three ϕ_3 values (unshaped, positive and negative TOD) is shown in Fig. 3. The diameter increases with pulse energy, however, the structure sizes created with pulses of both positive and negative ϕ_3 are smaller than those resulting from irradiation with unshaped pulses ($\phi_3 = 0$) at threshold.

In the case of pulses with GDD, the differences between positive and negative phase masks are not evident concerning the film modification threshold. Fig. 4 shows SEM images of a gelatine film irradiated with pulses with GDD $\phi_2 = \pm 1 \times 10^4$ fs^2 at the same distance to focus than those applied in the sample shown in Fig. 2a and b. When combining TOD and GDD masks, the observed effects are similar to the ones for irradiation with TOD shaped pulses alone, the modification threshold being higher for the cases when $\phi_3 < 0$.

4. Discussion

Laser induced foaming observed upon fs single pulse irradiation of biopolymer films has been reported before and ascribed to the increase of substrate temperature and to the evolution in the substrate of the laser-induced pressure wave. These give rise to nucleation and growth of bubbles and eventually to the formation of fibrillar structures or foam on the surface of the film [21,37]. The sudden heating induces the generation and propagation of a thermoelastic wave with a characteristic wave propagation time through the heated volume, defined as $\tau_m = 1/\alpha c_s$, where α is the absorption coefficient and c_s the sound propagation velocity ($\sim 1.5 \times 10^3$ m/s [21]). Under fs irradiation, and for these weakly absorbing materials, the condition for confinement of thermoelastic stress, $\tau_p/\tau_m < 1$, is well fulfilled, thus photomechanical effects play a definitive role in the observed material modifications [21].

As observed herein the modification threshold is achieved at lower pulse energies for positive ϕ_3 values for the same absolute value of the cubic phase. Thus, with pulses of identical fluence, spectrum and pulse duration, the different energy distribution in time has a significant influence on the material modification threshold. A commonly accepted prerequisite for surface modification or ablation upon fs laser pulse irradiation is the generation of a certain critical electron density [23,31]. The two main processes for generating free electrons are multi-photon ionization (MPI) and avalanche ionization (AI). MPI occurs on a time scale of a few femtoseconds, at a rate that is independent of the number density of free electrons (it requires no initial free electrons) and has highest efficiency for shortest pulses, i.e. highest intensities. In contrast, AI depends on the number density of free electrons and requires a longer time scale to develop. The process of AI can only contribute significantly for laser pulse durations in the femtosecond range after a large number density of free electrons has been provided by MPI.

Several authors have used rate equations based on the Drude model to describe the temporal evolution of the volumetric density of free electrons, ρ, and to calculate breakdown thresholds for various laser parameters [26,38]. The generic form of such a rate equation is

$$\frac{d\rho}{dt} = \eta_{mp} + \eta_{av}\rho - g\rho - \eta_{rec}\rho^2 \quad (1)$$

where the first and second terms on the right-hand side of the equation represent the production of free electrons through MPI and AI, while the last two terms describe electron losses through diffusion and recombination, respectively. The AI rate, η_{rec}, and the diffusion loss rate, g, are proportional to ρ, while the recombination rate, η_{av}, is proportional to ρ^2, as it involves an interaction between two charged particles (an electron–hole pair).

Previous studies on laser induced foaming of biopolymer films have shown that for unshaped pulses, the electron critical density is achieved via MPI processes [19,21]. A remarkable difference in the transient electron density generated in the medium as well as in the achieved final values, is revealed for both signs of the TOD ϕ_3. For $\phi_3 > 0$ (see Fig. 1), a strong pulse is followed by a train of weaker pulses. The amount of free electrons created by the first strong pulse via MPI is not sufficient for reaching the critical electron density value. However, the consecutive pulses can increase the electron density via AI to the critical density. For $\phi_3 < 0$ the intensity of the pulses increases and is terminated by a strong pulse. The first

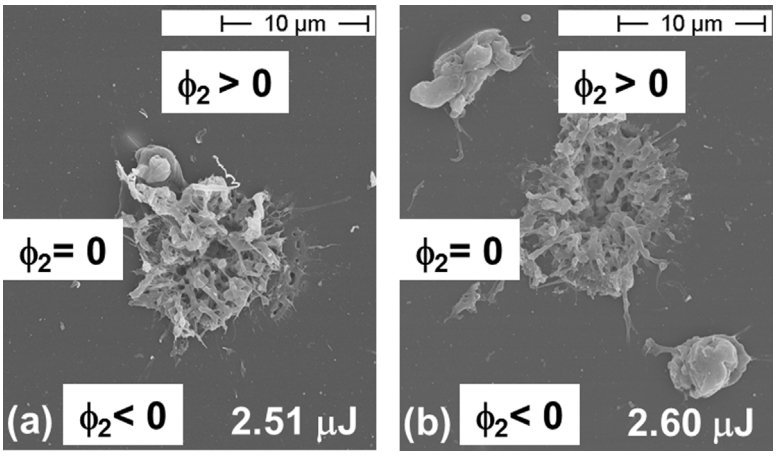

Fig. 4. SEM images of patterns obtained upon irradiation with GDD shaped pulses ($\phi_2 = \pm 1 \times 10^4$ fs^2) on a gelatine film with energies per pulse of 2.51 μJ (a) and 2.6 μJ (b) and same distance to focus.

weak pulses are not intense enough for efficient MPI and due to the absence of free electrons, AI is not operative either. Only the final pulse is able to deliver free electrons via MPI further increased by AI. For this case a higher energy is needed compared to the case of $\phi_3 > 0$ in order to reach the critical density, explaining the higher modification thresholds observed.

The absence of differences in the observed modification thresholds for GDD shaped pulses indicates that a change in frequency ordering within the same temporal envelope does influence the contributions from MPI and AI as seen also on dielectrics and water [39,40].

The smaller structure size obtained with modulated pulses could be also related to the different morphology observed when comparing the effect of temporally shaped and unshaped pulses. In the case of irradiation with unshaped pulses we obtain modified areas with a fibrillar-like structure, even at fluences close to the modification threshold, while irradiation with temporally shaped pulses gives rise to a swelling effect of the irradiated area. This is especially evident in the case of gelatine (Figs. 2a and b and 4) and could be explained by different propagation mechanisms. Upon irradiation with unshaped pulses, as previously reported [17,19,37], the confinement of thermoelastic stress gives rise to the evolution of the pressure wave in such a way that the nucleation and growth of bubbles cause the final fibrillar structure, via an explosive mechanism assisted by the tensile component of the laser-induced photoacustic transient wave. In the case of temporally shaped pulses, a different morphology has been observed in dielectrics and it was speculated that nanoplasmonic effects like near-field effects from a spatially confined region with high electron densities can be proposed as responsible for the observed steep hole structures [32]. On the other hand, since the temporally shaped pulses are effectively longer, the thermal diffusion and pressure lengths are larger, and the condition of confinement of thermoelastic stress is not so well fulfilled; instead, the pressure is only high enough in a small area where swelling takes place, but not reaching the values needed for explosive formation of the fibrillar/foam structure. This is more evident in the case of gelatine due to the nature of the biopolymer, as this material has a high water content, which on the one hand reduces the tensile strength of the substrate, facilitating bubble nucleation and growth, and on the other hand, in presence of water, laser energy is consumed as latent heat of evaporation contributing to suppression of increment of temperature in the irradiated region [37].

5. Conclusions

Laser irradiation of biopolymer films focused through a microscope objective using single femtosecond pulses of 790 nm leads to superficial foaming in a micrometer size region of the film. For gelatine and chitosan films the modification thresholds depend on the phase mask applied to the pulses, observing higher threshold values for temporally shaped pulses in comparison to the unshaped ones. When employing temporally asymmetric pulse shapes, higher modification thresholds were obtained in the case of negative phase masks. These differences are related to the different contribution of multi-photon and avalanche ionization processes. In contrast, the absence of differences in the observed modification thresholds for GDD shaped pulses is due to the symmetry of their temporal distribution. The results reported herein show a way to develop tailored pulse shapes for controlled superficial laser microstructuring of polymers.

Acknowledgements

Funding from MICINN, Spain (Project CTQ2010-15680), is gratefully acknowledged. E.R. thanks MICINN, Spain, for a Ramón y Cajal contract (RYC-2011-08069) and CSIC (PA1002917-Convocatoria estancias centros investigación extranjeros 2011). The Kassel group acknowledges financial support from DFG via the priority program SPP 1327.

References

[1] J.M. Perry, K. Zhou, Z.D. Harms, S.C. Jacobson, Ion transport in nanofluidic funnels, ACS Nano 4 (2010) 3897–3902.
[2] S. Xiao, V.P. Drachev, A.V. Kildishev, X. Ni, U.K. Chettiar, H.-K. Yuan, V.M. Shalaev, Loss-free and active optical negative-index metamaterials, Nature 466 (2010) 735–738.
[3] G.R. Hendrickson, M.H. Smith, A.B. South, L.A. Lyon, Design of multiresponsive hydrogel particles and assemblies, Advanced Functional Materials 20 (2010) 1697–1712.
[4] E. Rebollar, I. Frischauf, M. Olbrich, T. Peterbauer, S. Hering, J. Preiner, P. Hinterdorfer, C. Romanin, J. Heitz, Proliferation of aligned mammalian cells on laser-nanostructured polystyrene, Biomaterials 29 (2008) 1796–1806.
[5] A.C. Duncan, F. Rouais, S. Lazare, L. Bordenave, C. Baquey, Effect of laser modified surface microtopochemistry on endothelial cell growth, Colloids and Surfaces B: Biointerfaces 54 (2007) 150–159.
[6] H. Jiankang, L. Dichen, L. Yaxiong, Y. Bo, L. Bingheng, L. Qin, Fabrication and characterization of chitosan/gelatin porous scaffolds with predefined internal microstructures, Polymer 48 (2007) 4578–4588.

[7] J.G. Fernandez, C.A. Mills, J. Samitier, Complex microstructured 3D surfaces using chitosan biopolymer, Small 5 (2009) 614–620.
[8] W.-C. Hsieh, C.-P. Chang, S.-M. Lin, Morphology and characterization of 3D micro-porous structured chitosan scaffolds for tissue engineering, Colloids and Surfaces B: Biointerfaces 57 (2007) 250–255.
[9] N. Koufaki, A. Ranella, K.E. Aifantis, M. Barberoglou, S. Psycharakis, C. Fotakis, E. Stratakis, Controlling cell adhesion via replication of laser micro/nano-textured surfaces on polymers, Biofabrication 3 (2011) 045004.
[10] A. Ranella, M. Barberoglou, S. Bakogianni, C. Fotakis, E. Stratakis, Tuning cell adhesion by controlling the roughness and wettability of 3D micro/nano silicon structures, Acta Biomaterialia 6 (2010) 2711–2720.
[11] E. Stratakis, A. Ranella, C. Fotakis, Biomimetic micro/nanostructured functional surfaces for microfluidic and tissue engineering applications, Biomicrofluidics 5 (2011) 013411–013431.
[12] E. Stratakis, A. Ranella, M. Farsari, C. Fotakis, Laser-based micro/nanoengineering for biological applications, Progress in Quantum Electronics 33 (2009) 127–163.
[13] S.D. Gittard, R.J. Narayan, Laser direct writing of micro- and nano-scale medical devices, Expert Review of Medical Devices 7 (2010) 343–356.
[14] S. Lazare, V. Tokarev, A. Sionkowska, M. Wiśniewski, Surface foaming of collagen, chitosan and other biopolymer films by KrF excimer laser ablation in the photomechanical regime, Applied Physics A 81 (2005) 465–470.
[15] M. Oujja, S. Perez, E. Fadeeva, J. Koch, B.N. Chichkov, M. Castillejo, Three dimensional microstructuring of biopolymers by femtosecond laser irradiation, Applied Physics Letters 95 (2009) 263703.
[16] S. Gaspard, M. Oujja, C. Abrusci, F. Catalina, S. Lazare, J.P. Desvergne, M. Castillejo, Laser induced foaming and chemical modifications of gelatine films, Journal of Photochemistry and Photobiology A: Chemistry 193 (2008) 187–192.
[17] S. Gaspard, M. Oujja, R. de Nalda, M. Castillejo, L. Bañares, S. Lazare, R. Bonneau, Nanofoaming dynamics in biopolymers by femtosecond laser irradiation, Applied Physics A 93 (2008) 209–213.
[18] S. Lazare, Microfoams of biopolymers by laser-induced stretching: mechanisms and applications, in M. Elnashar, Biopolymers (2010) 109.
[19] S. Gaspard, M. Oujja, R. de Nalda, C. Abrusci, F. Catalina, L. Bañares, S. Lazare, M. Castillejo, Nanofoaming in the surface of biopolymers by femtosecond pulsed laser irradiation, Applied Surface Science 254 (2007) 1179–1184.
[20] S. Lazare, I. Elaboudi, M. Castillejo, A. Sionkowska, Model properties relevant to laser ablation of moderately absorbing polymers, Applied Physics A 101 (2010) 215–224.
[21] M. Castillejo, E. Rebollar, M. Oujja, M. Sanz, A. Selimis, M. Sigletou, S. Psycharakis, A. Ranella, C. Fotakis, Fabrication of porous biopolymer substrates for cell growth by UV laser: the role of pulse duration, Applied Surface Science 258 (2012) 9.
[22] L. Sudrie, A. Couairon, M. Franco, B. Lamouroux, B. Prade, S. Tzortzakis, A. Mysyrowicz, Femtosecond laser-induced damage and filamentary propagation in fused silica, Physical Review Letters 89 (2002) 186601.
[23] S.S. Mao, F. Quéré, S. Guizard, X. Mao, R.E. Russo, G. Petite, P. Martin, Dynamics of femtosecond laser interactions with dielectrics, Applied Physics A 79 (2004) 1695–1709.
[24] A. Vogel, V. Venugopalan, Mechanisms of pulsed laser ablation of biological tissues, Chemical Reviews 103 (2003) 577–644.
[25] A.-C. Tien, S. Backus, H. Kapteyn, M. Murnane, G. Mourou, Short-pulse laser damage in transparent materials as a function of pulse duration, Physical Review Letters 82 (1999) 3883–3886.
[26] M. Lenzner, J. Krüger, S. Sartania, Z. Cheng, C. Spielmann, G. Mourou, W. Kautek, F. Krausz, Femtosecond optical breakdown in dielectrics, Physical Review Letters 80 (1998) 4076–4079.
[27] M. Li, S. Menon, J.P. Nibarger, G.N. Gibson, Ultrafast electron dynamics in femtosecond optical breakdown of dielectrics, Physical Review Letters 82 (1999) 2394–2397.
[28] Y.P. Deng, X.H. Xie, H. Xiong, Y.X. Leng, C.F. Cheng, H.H. Lu, R.X. Li, Z.Z. Xu, Optical breakdown for silica and silicon with double femtosecond laser pulses, Optics Express 13 (2005) 3096–3103.
[29] R. Stoian, M. Boyle, A. Thoss, A. Rosenfeld, G. Korn, I.V. Hertel, Dynamic temporal pulse shaping in advanced ultrafast laser material processing, Applied Physics A 77 (2003) 265–269.
[30] L. Englert, B. Rethfeld, L. Haag, M. Wollenhaupt, C. Sarpe-Tudoran, T. Baumert, Control of ionization processes in high band gap materials via tailored femtosecond pulses, Optics Express 15 (2007) 17855–17862.
[31] L. Englert, M. Wollenhaupt, L. Haag, C. Sarpe-Tudoran, B. Rethfeld, T. Baumert, Material processing of dielectrics with temporally asymmetric shaped femtosecond laser pulses on the nanometer scale, Applied Physics A 92 (2008) 749–753.
[32] L. Englert, M. Wollenhaupt, C. Sarpe, D. Otto, T. Baumert, Morphology of nanoscale structures on fused silica surfaces from interaction with temporally tailored femtosecond pulses, Journal of Laser Applications 24 (2012).
[33] A.M. Weiner, Femtosecond pulse shaping using spatial light modulators, Review of Scientific Instruments 71 (2000) 1929–1960.
[34] A. Assion, M. Wollenhaupt, L. Haag, F. Mayorov, C. Sarpe-Tudoran, M. Winter, U. Kutschera, T. Baumert, Femtosecond laser-induced-breakdown spectrometry for Ca^{2+} analysis of biological samples with high spatial resolution, Applied Physics B: Lasers and Optics 77 (2003) 391–397.
[35] M. Wollenhaupt, A. Assion, T. Baumert, Femtosecond laser pulses: linear properties, manipulation, generation and measurement, in: F. Träger (Ed.), Handbook of Lasers and Optics, 2007.
[36] J.D. McMullen, Chirped-pulse compression in strongly dispersive media, Journal of the Optical Society of America B 67 (1977) 1575–1578.
[37] S. Lazare, R. Bonneau, S. Gaspard, M. Oujja, R. De Nalda, M. Castillejo, A. Sionkowska, Modeling the dynamics of one laser pulse surface nanofoaming of biopolymers, Applied Physics A 94 (2009) 719–729.
[38] B.C. Stuart, M.D. Feit, S. Herman, A.M. Rubenchik, B.W. Shore, M.D. Perry, Nanosecond-to-femtosecond laser-induced breakdown in dielectrics, Physical Review B 53 (1996) 1749–1761.
[39] M. Wollenhaupt, L., Englert, A. Horn,T. Baumert, Temporal femtosecond pulse tailoring for nanoscale laser processing of wide-bandgap materials, Proc. of SPIE 7600 (2010) 7600X.
[40] C. Sarpe, J. Köhler, T. Winkler, M. Wollenhaupt, T. Baumert, Real-time observation of transient electron density in water irradiated with tailored femtosecond laser pulses, New Journal of Physics 14 (2012) 075021.